PLANTMASS MEDIATED SYNTHESIS OF METAL TUNGSTATE NANOPARTICLES: A SHOT REVIEW ON ITS SYNTHESIS, CHARACTERIZATION, AND PHOTOCATALYTIC APPLICATIONS

Abstract

Recently, metal oxide nanoparticles (NPs) have been shown to have substantial commercial potential. The intrinsic qualities of nanomaterials, such as their exact size, shape, composition, increased surface-to-volume ratio, and purity of individual components, make them intriguingly adaptable materials. This paper presents a full explanation of contemporary green synthesis research that is more advantageous than traditional chemical synthesis in terms of cost, pollution reduction, and environmental and human health safety. In particular, the role of Tunstate nanoparticles (NPs) as photocatalysts has gained great interest because of their potential electronic structural configuration, light absorption capabilities, and charge transport characteristics. Plant-based green technologies have been created for the production of nanoparticles because to the high concentration of hazardous substances and the harsh conditions utilised in chemical and physical processes. The definition of metal oxides as photocatalysts, their structural characteristics, the prerequisites for photocatalysts, the classification of photocatalysts, and the mechanism of the photocatalyst are all covered in this article. The diverse life on our planet is in grave risk from water contamination caused by many substances like metal ions, textile dyes, medical waste, other residential activities, and industrial operations. Numerous methods are used for purifying water that is contaminated, notably adsorption, ion exchange, flotation, coagulation-flocculation, electrochemical precipitation, chemical precipitation, and reverse osmosis. The

Authors

R. Karthiga
PG and Research Department of Chemistry
Cardamom Planters' Association College
Bodinayakanur, Theni, Tamilnadu, India.

S.Karthikarani
Department of Physics
Cardamom Planters' Association College
Bodinayakanur, Theni, Tamilnadu, India.
skarthika1121@gmail.com

T. Pandimeena
Department of Physics
Cardamom Planters' Association College
Bodinayakanur, Theni, Tamilnadu, India.

development of new and improved processes that boost the effectiveness of water treatment depends significantly on nanotechnology. Since oxides of metals act as a diverse group of nanomaterials, extensive research is being done to figure out them and use them to purify contaminated water of contaminants. This review studies photocatalytic wastewater treatment using different metal oxide nanoparticles. The influence of several particular characteristics such as the catalyst synthesis technique, the starting dye concentration, the quantity of nanocatalyst needed for degradation, the initial pH of the dye solution, the kind of light source employed, and the exposure period. Special emphasis was given to the light required to remove the dye. Based on a preliminary study of the extant literature, some broad findings were reached. The study compares suspended and supported catalysts in-depth, discusses their general/specific requirements, key factors affecting degradation, and performance evaluation methods. In order to attain increased removal effectiveness in an efficient fashion, several appropriate test conditions must be adopted to breakdown these resistant dyes. Future research directions are also given.

Keywords: green synthesis, degradation, metal tungstate, doping, coupling.

I. INTRODUCTION

One of the ideas that has advanced the fastest in recent years is nanotechnology, which has brought great technological as well as scientific breakthroughs. A range of new systems, structures, devices, and nanoplatforms with potential applications could be developed created using nanomaterials with distinctive physicochemical properties [1], [2]. In contrast to their enormous surface area and volume, nanomaterials have increased thermal conductivity, catalytic reactivity, nonlinear optical efficiency, and chemical stability [3]. Plenty of researchers have been motivated to look for novel synthesis techniques by this feature. Although conventional methods (physical and chemical processes) take less time to create a large number of nanoparticles, they call for toxic materials like preservatives to maintain their stability, which is toxic to the environment. Considering this, plant-based green technology is gaining popularity as an environmentally friendly, non-toxic, and safe alternative, because the green synthesis of nanoparticles mediated by plant extracts is economically favourable, and provides natural coatings in the form of proteins[4], and allows the careful synthesis of different shapes and sized nanoparticles. Biomass of plant is used to synthesis nanoparticles is a trending way to generate nanoparticles employing biologically derived substances.

This review discusses traditional synthetic methodologies with an emphasis on current improvements in synthesis methods for greener metals, metal oxides, and other relevant NPs. The methods and environmental factors that affect the surface shape, degradability, and other characteristics of these green synthetic NPs are subsequent studied. An evaluation of the current status and future prospects in the synthesis of nanoparticles using various green technologies concludes the study. This study focuses on novel and enhanced environmentally friendly synthesis techniques for metal oxide nanoparticles that are responsive to a variety of stimuli, producing outstanding and cost-effective nanomaterials [5], that can be used in a variety of applications and are biodegradable. This environmentally friendly synthesis not only creates incredibly efficient nanocarriers, but also accomplishes its goals without endangering the environment or other living things.

Green chemistry is employed in the biological synthesis of NPs because it is non-toxic, ecologically friendly, and energy efficient. The fundamentals of green chemistry, including preventative, safer chemical synthesis, the use of renewable raw materials, reducing derivatives, etc., emerged as a consequence of biological synthesis. From the biological approach, NPs are created from sources such as fungi, bacteria, plants, animals, etc. Biological sources demandsmore expensive strategies like culture maintenance and microbial separation but plant extracts offers more advantages for the synthesis of nanoparticles [6]. The secondary metabolites present in the plant extract (Alkaloids, proteins, carbohydrates, enzymes, phenolic acids, and other substances) act as a stabilising and reduction processes.The secondary metabolites as biological substrates which reduce the need for chemicals to make metal nanoparticles from the precursor solutions since they contain so many essential phytochemicals. [7]. Leaf extracts are commonly employed in green synthesis since leaves contain various metabolites, and this process is safe, biocompatible, and ecologically beneficial[8], [9].

Rapid industrialization, new development processes, and a rising population have continually harmed the global environment [10], [11]. Organic pollutants from diverse sources such as industry, agriculture, and chemicals have seriously contaminated water, which creates a hazard to people and aquatic life [12].Organic dyes have been widely tapped across multiple fields of study, such as large scale industries like textile, leather, paper, and pulp and end up in organic effluent.Several studies have been carried out on the degradation of these organic dyes under the effect of photocatalysts[13–15], however, there are various approaches to obtain the ultimate solution.

Beneath the impact of ultraviolet (UV) or visible wavelengths, the catalyst is utilised to accelerate the chemical reactions of the photocatalyst. The phrases "photo" and "catalysis" derive from ancient Greek. In photocatalysis light is the "photo" which speeds up the rate of the reaction by using an external material ("catalyst") which is not itself consumed in the process. A catalyst lowers the activation energy needed for a chemical reaction and speeds up the process. So far, there are three different methods to create visible light photocatalysts: (i) generate a donor level above the valence band by doping some elements with wide-gap semiconductors in typical photocatalysts, (ii) create a new valence band using some elements, (iii) manage the band structure by generating the solid solution shown in Fig. 1. Recently there have been many studies on the second strategy and new materials such as $SrWO_4$[16], Tb_3 /$La_2(WO_4)_3$[17], $BiWO_4$[18],$MnWO_4$[19], WO_3/g-C_3N_4/V_2O_5[10], WO_3[20]. WO_3 is an excellent photocatalytic material and is directly connected to visible light photocatalytic materials. Due to faults in the production process of WO_3, the material is somewhat biased towards n-type semiconductors.

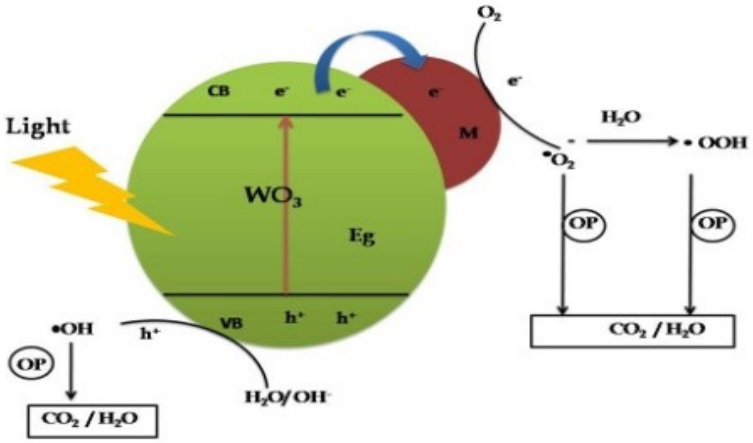

Figure 1: Mechanism of photodegradation of WO_3 with metal doping

Since WO_3 has an experimental bandgap energy (E_g) of 2.5 to 3.0 eV, it is possible that it can absorb the majority of visible light in the range of 380 to 700nm as a photocatalyst. The band gap of several metal tungstates is given in Fig. 2. [21].The formation of pairs of electrons and holes under light is one of the properties of the material as a photocatalyst. The recombination duration of this pair is longer with a capable photocatalyst. In addition, these electron and hole pairs form hydroxyl radicals (OH^-) and superoxide

radicals (O_2^-), which have been proved to be good scavengers for the photocatalytic elimination of harmful dyes.

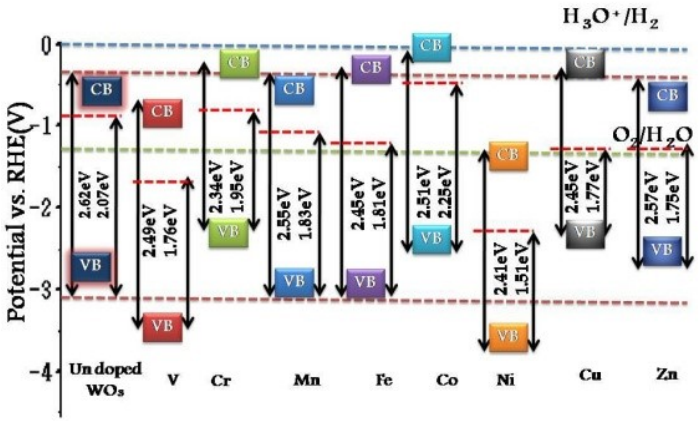

Figure 2: Band gap of transition metal tungstate

1. **Schematic Mechanism for Coloured Pollutant Degradation:** In the visible light region photocatalytic dye degradation because of their propensity to absorb part of the visible light. The excitation of coloured pollutants in a visible light photon ($\lambda > 400$ nm) from the valance band (Coloured pollutant) to the Conduction band (triplet excited state of Coloured pollutant *). Cation of half-oxygenated is generated from excited state of dye (Turkture) by electron injection into the conduction band of Nanoparticles [22]. Hydroxyl radicals ($OH^{\cdot}$) are generated by the interaction between these trapped electrons and oxygen dissolved in the system, superoxide radical anions ($O_2^{-\cdot}$). Fig 3 and the equation shows the OH radicals are largely responsible for the oxidation of the organic compounds [8], [23].

   Coloured pollutant + hν → Coloured pollutant *
   Coloured pollutant * + NPs → Coloured pollutant $^+$ + NPs $^-$

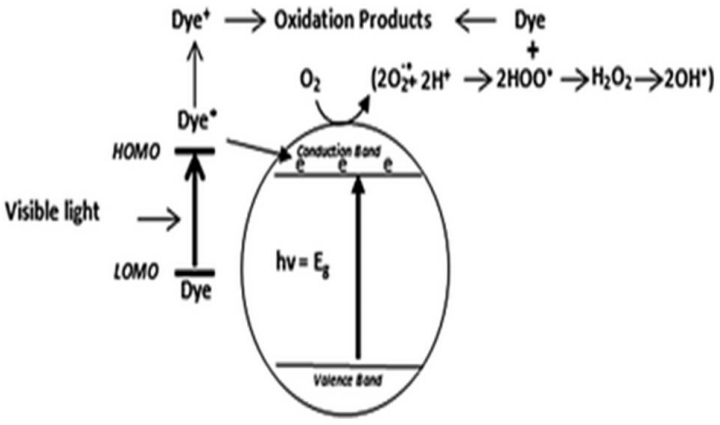

Figure 3: Mechanism of oxidation of the organic compounds using $OH^{\cdot}$ radicals

2. **Advantages of Green Synthesis:** Hazardous, expensive, and deadly chemicals are used as reduction agents. Green synthesis that is simple, affordable, and effective as a stabilizer is desperately needed. The existence of bioactive substances (i.e., secondary metabolites of plants such as terpenoids, phenols, alkaloids, flavonoids, quinines, or tannins), which not only have antibacterial and antioxidant properties but also reduce metal ions and stabilize nanoparticles [24]], which create a stable protective barrier for Metal oxide nanoparticles and thereby prevent Metal oxide nanoparticles from aggregating, is primarily responsible for the practical use of the above method [25].

According to the growing acceptance of green approaches, numerous ways have been devised to generate WO_3 Nanoparticles from diverse sources such as bacteria, fungus, algae, plants, and others. A collection of tables has been prepared to highlight works in this area (Table 1).

Table 1: List of nano tungstates synthesized by different plant extract and their size and shape

S.no	Plant	Tungstates	Size	Shape	Reference
1	Gelatin	WO_3	40	Hexagonal crystal	[26]
2	Rhamnusprinoides	WO_3	60	Spherical shape	[27]
3	Spondiasmombin	WO_3	5.90	Agglomerated	[28]
4	Agar-agar from red seaweed	$CoWO_4$	84.3	Strong agglomeration	[29]
5	Red algae(Rhodophyta).	$CoWO_4$	13-30	Nanospheres	[29]
6	Aloe vera	$FeWO_4$	15.83	Nanorods	[30]
7	Brassica rapa	$CdWO_4$	27	Rod shape	[31]
8	Azadirachtaindica	$NiWO_4$	31.1	Agglomerated	[32]
9	Phyllanthus Amarus	$NiWO_4$	33.49	Flower	[33]
10	Hyphaene thebaica L	$ZnWO_4$	24	Rod	[34]
12	Lemon	ZnO-$CuWO_4$	97.70	Agglomerated	[35]
13	Starch	TiO_2–Bi_2WO_6	13.5	Nanoplates	[36]
14	Lignin	Ni-$CoWO_4$	-	Disordered plate	[37]

II. TUNGSTATE

1. **Tungstate for Detectionof Toxicity**: Tungsten oxide nanosheets were synthesised by Ghazal et al. described the sol-gel process. For the manufacture WO_3, Na_2WO_4 as a metal precursor and gelatin solution as a novel green stabilizer. This is characterized by XRD, FESEM/EDX, Raman, UV and vis.DRS. Photocatalytic experiments were carried out using WO_3-Nanosheets (650 °C) for the optical degradation of the dye at the surrounding

temperature using a mercury vapour lamp (50 W) at high-pressure was employed. It analyses the elimination of MB dye at 95% in 187 minutes by degrading the organic portion of the dye. This finding demonstrated the great predilection of these nanoparticles for the removal and degradation of pigments, whose reaction kinetics were shown to be practically first order. In addition, WO_3-NS ceased cytotoxicity in Huh-7 cells and demonstrated low cytotoxicity, showing the biocompatibility of the nanosheets at high concentrations. Huh-7 cells showed great resistance in the MTT test, although identical results were seen even at high dosages up to 31 g/ml.

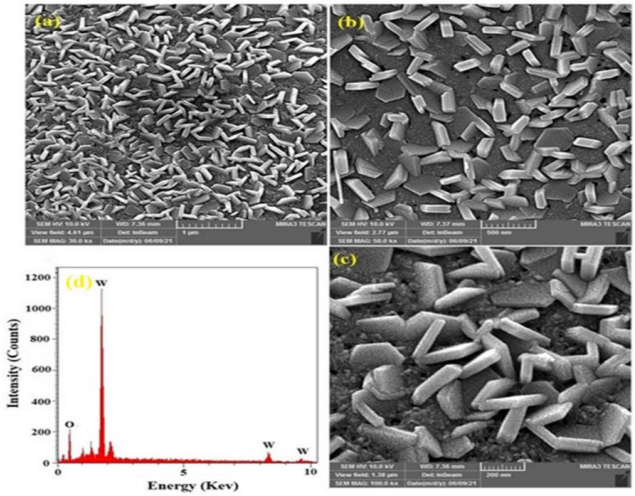

Figure 4: FE-SEM image of WO_3-NS calcined at 650◦C[26]

2. **Tungstate for Antibacterial Performance:** Rhamnusprinoides extract of leaves and sodium tungstate precursor were employed to prepare tungsten trioxide nanoparticles with a monoclinic shape for investigating their potential as antibacterial agents. The author studied the synthesised WO_3 using X-ray diffraction (XRD), scanning electron microscopy (SEM) and Fourier transform infrared spectroscopy (FTIR) to study its antibacterial activity. At a dosage of 250 mg/ml and 125 mg/ml the synthesised WO_3 nanoparticles showed amazing antibacterial activity. As demonstrated in Fig. 5, the inhibition zones of Listeria monocytopens (Lm), Staphylococcus aureus (Sa), Salmonella typhimurium (Sa), Escherichia coli (Ec) and Candida albicans (Ca) were analysed [38], [39]

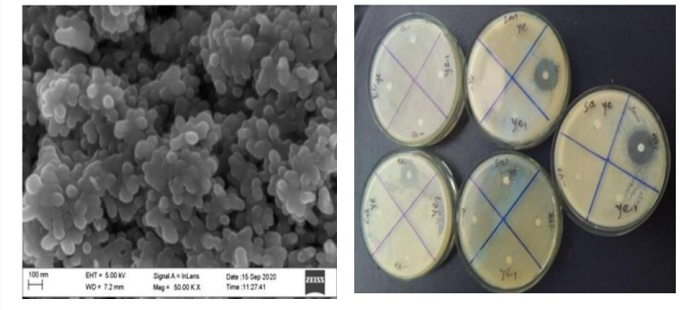

Figure 5: SEM and Antibacterial activity of WO_3[27]

3. **Tungstate for Structural Research through pH:** By combining ammonium paratungstate, $(NH_4)10W_{11}O_{41}•5H_2O$), with an aqueous extract of spondiasmombin, Tijani et al. attempted to produce WO_3 nanoparticles with controlled form and size [28]. The morphological arrangement and structural properties, such as the average crystallite size and surface area, were additionally strongly affected by the solution pH and calcination temperature [40, 41].]. It was previously proven that crystallite sizes increase with solution pH and calcination temperature. There was no change in the WO_3 phase type at the used calcination temperature and pH, and solely the monoclinic polymorph was produced [42]. The aqueous spondiasmombin biomolecules binding, and stabilizing actions in the produced WO3 nanoparticles may also be significant for the observed shape. The particle size of WO_3 nanoparticles was shown to generally increase in the range of 13.8 to 14.3 to 16.7 nm, and 1, 4, 7, and 10 in the order of pH, respectively. Acidic conditions promote WO_3 pristine monoclinic symmetry. The successful synthesis and monoclinic phase formation of WO_3 nanoparticles with a higher specific surface area and small crystal size compared to other manufacturing techniques found in the literature were confirmed by all characterization techniques used in this work, and their SEM image was shown in Fig. 6.

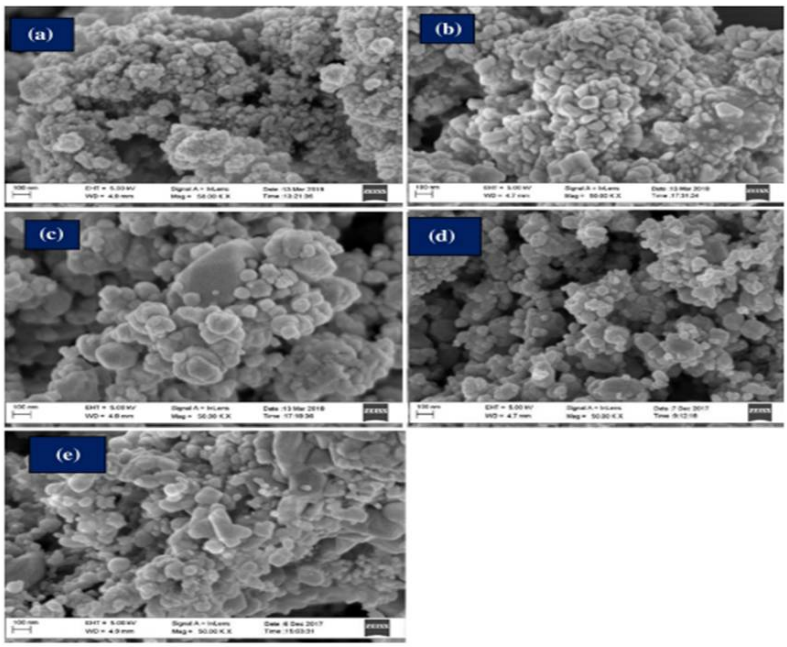

Figure 6: HRSEM images of WO_3 nanoparticles generated at optimal pH of 1 and calcined at temperature (a) 250 °C, (b) 350 °C,(c) 450 °C, (d) 550 °C, and (e) 650 °C withcontinuous holding time of 2 h[27]

III. TRANSITION METAL DOPED TUNGSTATE

1. **Prolonged Durability of Electrodes by Cobalt Tungstate:** The author offers a protein sol-gel green method for synthesizing cobalt tungstate ($CoWO_4$) powders for electrodes that resemble batteries using red algae (Rhodophyta) agar. In contrast, $CoWO_4$ is produced using flavorless gelatin and comparable protein chemistry. The resultant powders were then calcined at 800 °C for 2 hours to analyze the battery-like behavior in

an alkaline environment (3 MOH) utilizing XRD (Rietveld refinement), SEM/EDS, FTIR/Raman/UV-Vis-NIR spectroscopy, VSM, and many electrochemical experiments. The data show that samples made with gelatin had an average particle size of 150 nm and a crystallite size of 68 nm, while the agar-agar-treated materials had particle sizes of 284 nm and crystallite sizes of 84 nm. The paramagnetic behaviour of these samples was confirmed by magnetic testing at 300 K. An examination of samples taken at 4.926 m along these curves revealed that the effective magnetic moment for each cobalt atom in gelatin and agar was 4.908 m and 4.908 m, respectively. The surface faradic Redox reaction mechanism and the reversible valence state between CO_2 and CO_3 are both credited with $CoWO_4$ effectiveness as a battery-like electrode. The discharge curves, which have a maximum specific capacity of 77 C g^{-1} and a maximum specific current of 1 A g^{-1}[43]. Show no discernible variations in electrochemical activity. The capacity retention of almost 98% through 1000 charge-discharge cycles at 1 A g^{-1} was presented in Fig. 7 [44] as evidence of the electrodes' long-term durability.

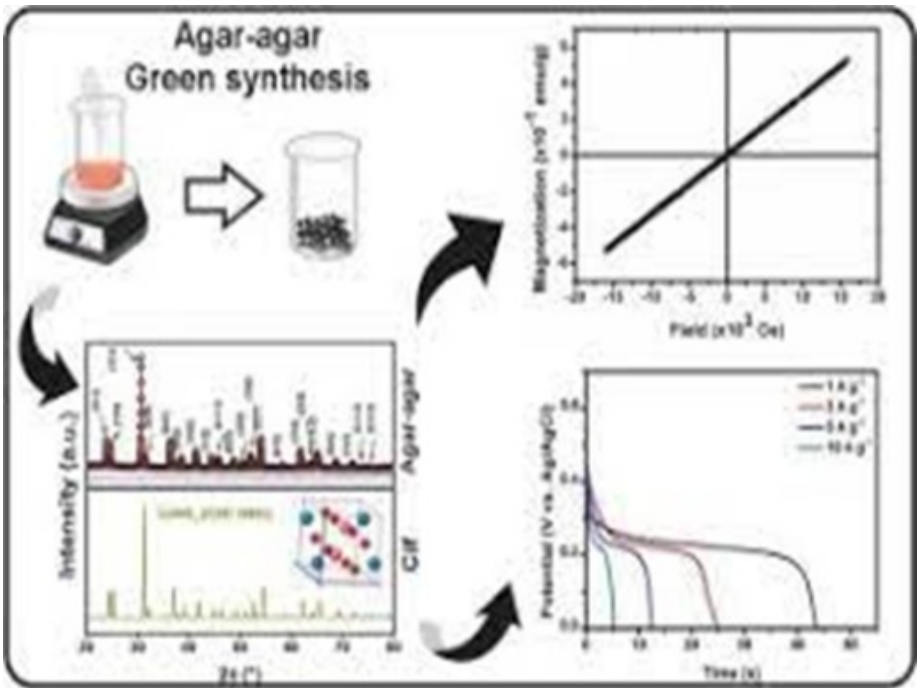

Figure 7: Graphical abstract for capacity retention and charge-discharge cycles of cobalt tungstate[29]

2. **Iron Tungstate for Selective Determination of Theophylline:** Theophylline can be detected selectively and sensitively employing Aloe Vera extract from plants coated iron tungstate nanorods (AFW) immobilised Nafion (Nf) modified glassy carbon electrode (GCE) (AFW/Nf/GCE), according to the author [30]. Co-precipitation was used to generate AFW that was then analysed using a number of techniques, namely elemental analysis (EDX), scanning electron microscopy (SEM), X-ray diffraction (XRD), Fourier transform infrared spectroscopy (FT-IR), and electrochemical tests. Comparing theophylline oxidation on AFW/Nf/GCE to bare GCE and iron tungstate (FW) modified GCE, it is interesting to note that the former showed increased electrocatalytic activity. 0.0028 mM was fixed as low limit of detection (LOD) of theophylline oxidation in the

electrochemical sensor also demonstrated a linear response range from 0.1 to 160 mM [45]. As can be seen in Figure 9, this sensor demonstrated excellent selectivity, stability, and reproducibility in the biological and food samples under study. It has been successfully used to identify theophylline specifically in urine, black tea, and human serum samples.

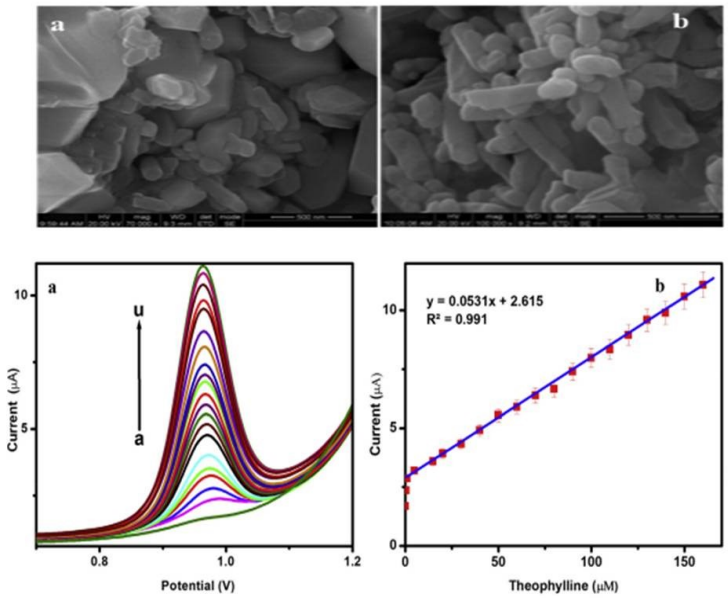

Figure 8: SEM images for a) iron tungstate and b) aloe vera plant decorated iron tungstate, Fig.9 (a) shows the AFW/Nf/GCE's DPV response in 0.1 MPBS (pH 7.0) with theophylline concentrations ranging from 0.1 to 160 μM, and (b) shows the inset calibration plot showing the linear relationship between peak current and theophylline concentration.

3. **Bismarck brown R photodegradation of Via Brassica rapa leaf of $CdWO_4$:** Brassica rapa leaf extract was utilized by Fatima et al., to synthesis $CdWO_4$ via in situ functionalized for adsorption of Bismarck brown R rod-shaped f-$CdWO_4$ and for photocatalytic activity. 54 nm of average particle size was found for $CdWO_4$ using XRD and TEM imaging. The length and average width of the nanorods were both 120 nm. Considering the various parameter like dosage, concentration, contact time, pH, reaction temperature, for batch adsorption test. In 15 minutes, 1.5 gL^{-1} of f-$CdWO_4$ was able to remove 80% of Bismarck brown R dye from an initial concentration of 10 mgL^{-1}. At an acidic pH, the improved adsorption capacity of f-$CdWO_4$ was optimised. At 30 °C, f-$CdWO_4$ had the highest Langmuir adsorption capacity at 46.5 mg^{-1}. The surface functionalization of $CdWO_4$ was blamed for the improved absorption capability of Bismarck brown R f-$CdWO_4$. Excellent photocatalytic activity towards Bismarck Brown R was also shown by f-$CdWO_4$. The degradation process of Bismarck brown R is shown in Fig. 10. $CdWO_4$ for adsorption and photocatalytic activity for the Bismarck brown R.

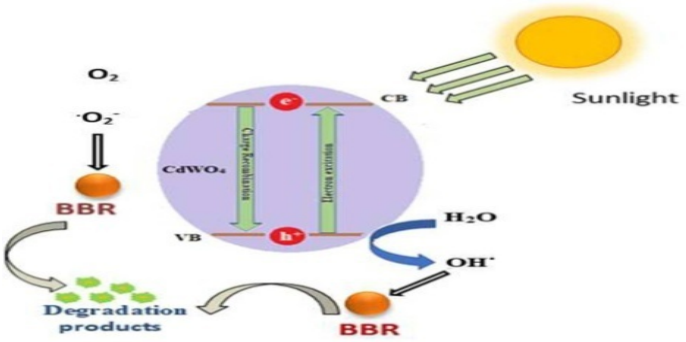

Figure 10: Proposed simplified degradation scheme of Bismarck brown R

4. **Nickel Tungstate for Photocatalytic Activity of Dye:** Particles of nickel tungstate ($NiWO_4$) altered with Azadirachta indica extract of plants were synthesised by a co-precipitation technique developed by Karthiga et. al [32]and others and characterised by UV-vis-DRS, FT-IR, XRD, SEM, TEM and EDX techniques and SEM findings suggested that the plant extract altered $NiWO_4$ included of tiny spheres in Fig. 11. Based on XRD observations, bare $NiWO_4$ created through the co precipitation approach had an average crystallite size of 31.11 nm, whereas $NiWO_4$ infused with plant extract exhibited a smaller average crystallite size of 12.12 nm. Methylene blue (MB) was used as a model organic polluter for the investigation of $NiWO_4$ nanoparticles photocatalytic activity [46] under visible light illumination. At a PNT dosage of 0.05 g/L and an MB concentration of 10 µM, optimal photodegradation is reached after 180 minutes under tuned reaction conditions. According to Fig. 12, PNT was more effective than Gram (+ve) and Gram (-ve) microorganisms.

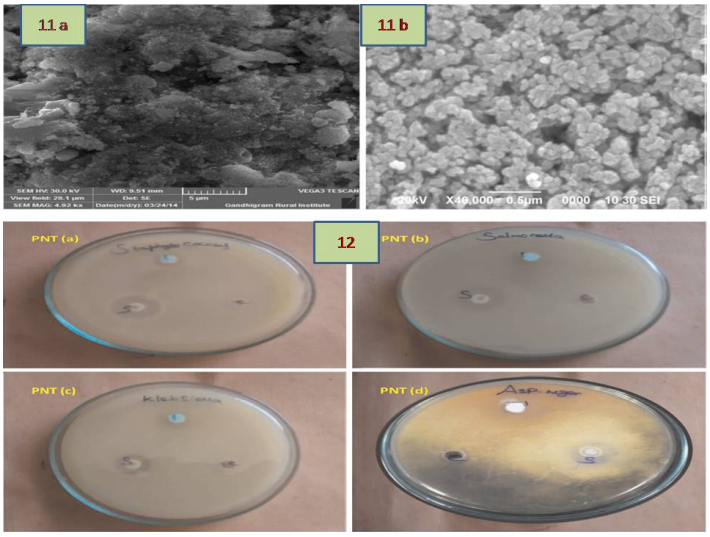

Figure 11: SEM image of $NiWO_4$ and plant extract modified $NiWO_4$, Fig. 12. The zone of inhibition of PNT against (a) Staphylococcus, (b) Salmonella (c) Klebsiella (d) Aspergillus niger[47]

5. **$ZnWO_4$ for the visible light photocatalytic activity of dye:** Fig. 13 shows how Hyphaene thebaica fruit extract can be used to produce zinc tungstates via green chemistry, according to K. Hkiri et al. The biosynthesized powder was found to have good crystallinity and to be completely free of impurities and secondary phases, based on structural analysis. Numerous elements with oxygen vacancies were discovered by RBS spectroscopy, which is in perfect accord with both the EDS and anticipated outcomes. Scanning and transmission microscopes were used for the morphological analysis, which revealed that the zinc tungsten was made up of spherical nanoparticles that were evenly distributed and contained some rod-like particles [34], [48]. To assess the photocatalytic efficiency of biosynthesised $ZnWO_4$, MB was employed as an organic dye. Under visible light irradiation, a series of reactions with various starting concentrations were carried out using a 1 g/L $ZnWO_4$ catalyst. As the initial dye concentration increased from 1.10^{-5} mol/L to 3.10^{-5} mol/L, the degradation efficiency of MB fell from 98.4% at 90 min to 90% at 270 min. The principal reactive species involved in the photodegradation of MB dye are O_2 and $OH^{\cdot}$ radicals, according to data on scavenger activity. On the basis of experimental and theoretical evidence, a fictitious reaction mechanism was used to explain the photodegradation of MB on zinc tungsten photocatalysts. It was demonstrated that oxygen vacancies can increase the photocatalytic energy by producing more oxidised groups and preventing electron-hole recombination (Fig. 14), in addition to lowering the energy needed for the electronic transition from VB to CB by forming defective energy levels in the $ZnWO_4$ band gap. Therefore, oxygen vacancies should be responsible for the increased visible light absorption of biosynthesized $ZnWO_4$. Recycling experiments showed persistent photocatalytic activity of $ZnWO_4$ produced through green chemistry. As a result, a $ZnWO_4$ catalyst that may be used as a photocatalytic catalyst for pollutant degradation may be produced by a fruit extract of Hyphaene thebaica.

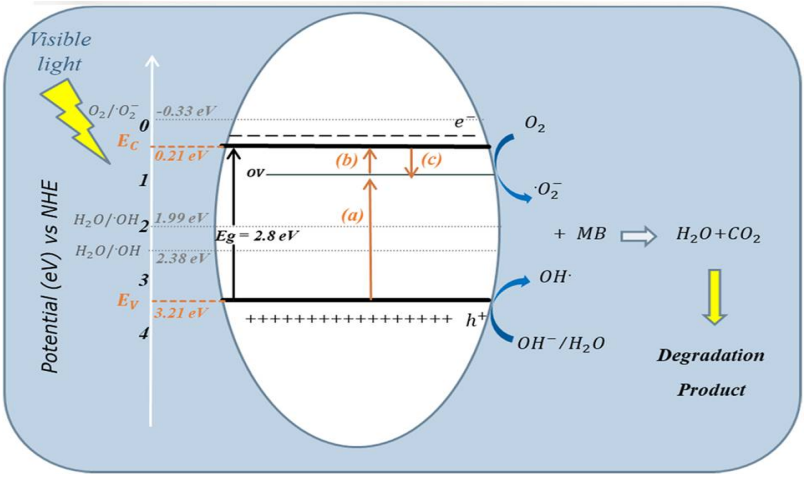

Figure 14: Photocatalytic degradation methylene blue mechanism of $ZnWO_4$[49]

IV. COUPLING

1. **ZnO-$CuWO_4$ for Environmental and Biological Fields:** The leaf extract was used as a reducing, capping, and stabilising agent for generation ZnO-$CdWO_4$ nanoparticles. The phytochemical on the surface of the nanoparticles gives rise to number of functional sites on the adsorbent surface, increasing the adsorption capacity. Freundlich isotherm model,

spontaneity and exothermic were used to estimated ΔG^o, ΔS^o and ΔH^o values, which show the best fit of the CR adsorption to the pseudosecondary kinetic model by a chemisorption mechanism (Fig. 15). Electrostatic and hydrogen bonding during CR absorption was explained by FT-IR and also the shape of the ZnO-$CdWO_4$ surface. Using interparticle diffusion and Boyd plots, researchers highlighted the actual rate-determining phase in the CR adsorption process. The basic regulation of the CR molecule adsorption on the ZnO-$CdWO_4$ surface was thus revealed by the intraparticle diffusion mechanism [50]. Because of this, the utilisation of ZnO-$CdWO_4$ NPs in this study for the adsorptive removal of Congo red is a brand-new and exciting method for treating water. Pollutant co-existence may have decreased CR dye adsorption removal due to the dominance of competing adsorption processes. Because of the synergistic interaction between metal oxides and phytochemicals from plants, ZnO-$CdWO_4$ is a promising contender for both environmental and biological applications. More research is required to determine its potential as a photocatalyst, antioxidant, antibacterial, and anticancer agent. In conclusion, it was found that ZnO-$CdWO_4$ produced via green synthesis is a cost-efficient, highly efficient, and sophisticated material to address numerous environmental issues.

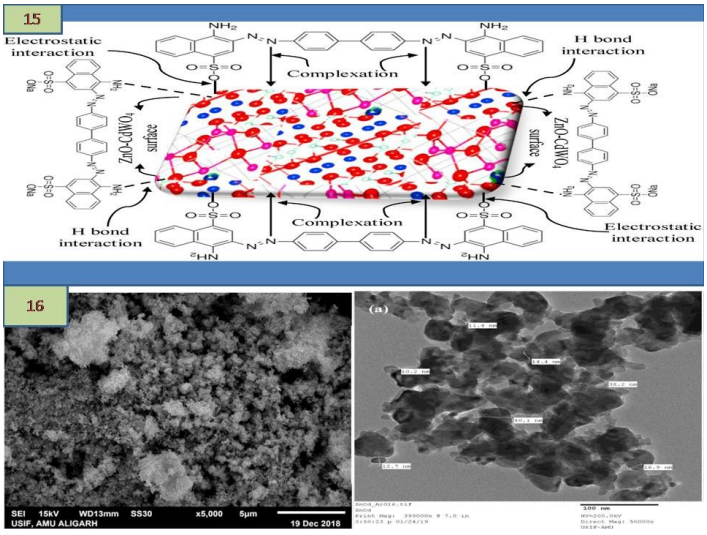

Figure 15: Scheme for various reduction of dye[51], Fig .16. SEM and TEM image of ZnO-$CdWO_4$Nanocomposite

2. **TiO_2/Bi_2WO_6 Photocatalytic Processing of Biomass:** This research examines a novel photocatalytic technique to reduce complicated biomass into smaller molecular units for use in the manufacturing of biofuel feedstocks[52]. After the hydrothermal process, the TiO_2-Bi_2WO_6 nanocomposite photocatalyst was employed for various TiO_2 ratios, viz. 15 and 25 wt% was created. The photodegradation efficiency of the organic molecule is determined. The composite loaded with 25% TiO_2 was determined to represent a maximum photocatalytic efficiency of 99.9%. The structural and optical characteristics of the produced photocatalytic nanomaterial were studied.Rhodamine B elimination in Fig.17 revealed a band gap of 2.7 eV for the 25% TiO_2 composite with remarkable visible light photoactivity. Additionally, we find that this combination has four times the photocatalytic activity of pure Bi_2WO_6[53]. A biopolymer, usually starch, is

photocatalytically fragmented using this chemical to create smaller molecular precursors. Starch monomerization is discovered through a colorimetric analysis of reducing sugars from decomposing biomass. The produced linear chain's molecular fragments underwent additional Raman, FTIR, and ESI-MS analysis. The results show that TiO_2/Bi_2WO_6 nanocomposite photocatalytic pretreatment of starch results in the formation of organic precursors, which are typical raw materials for anaerobic methanation and ethanol fermentation microorganisms. As a result, we draw the conclusion that the processes of biomass hydrolysis and partial acetogenesis can both benefit from biomass photocatalytic pretreatment. This idea offers a sustainable method of turning biomass waste into biofuel[36].

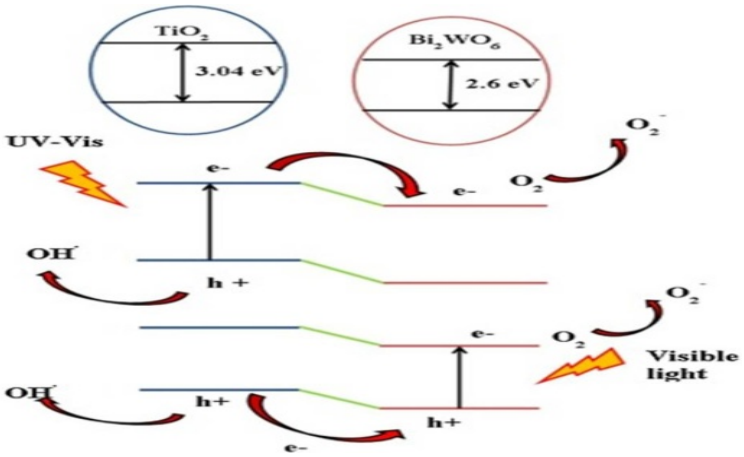

Figure 17: Mechanism of photodegradation of TiO_2–Bi_2WO_6[36]

V. BIMETAL DOPING USING TUNGSTATE

1. **Ni-$CoWO_4$ for Electrochemical Application:** This investigation examines the function of lignin functionalized (M_2) in the bimetallic tungsten compounds ($M_2M_1WO_4$, M_2 = Ni, M_1 = Co. A high SPC value of 862.26 mF cm^{-2}, which was 141 times bigger than the monometallic tungsten ($CoWO_4$) functionalized lignin supercapacitor's SPC value of 6.1 mF cm^{-2}, was found to exist in the bimetallic tungsten ($NiCoWO_4$) functionalized lignin supercapacitor[37].Due to the larger oxidation state that is accessible in the bimetallic tungsten secondary metal M_2 ($M_2M_1WO_4$, M_2 = Ni, and M_1 = Co), the pseudo capacitance is significantly increased, which improves electron conductivity. Due to the combined effects of lignin-encapsulated bimetallic tungsten NPs, the lignin/$NiCoWO_4$ supercapacitor also exhibits the highest energy density of 5.75 Wh kg^{-1} and the highest power density of 854.76 kW kg^{-1}. The capacitance retention increased as the fraction of bimetallic tungsten NP in the composite electrode grew. The retention was 100% even after 2000 cycles at the optimal lignin: $NiCoWO_4$: PVDF mass ratio (15:75:10), and their morphological investigations are presented in Fig. 18. An examination into supercapacitor discharge times showed that retention was increased at shorter discharge intervals and considerable SPC at longer discharge periods. As a result, $NiCoWO_4$ pseudocapacitive nanomaterial's electroactive site consumption rate was inversely proportional to discharge time. Lignin's molecular structure is changed by carbonation, which results in high charge transfer impedance and decreased electrochemical efficiency

[54]. It has been shown that the capacitive performance of the bimetallic tungsten supercapacitor is significantly influenced by the choice of the negative electrode's surface area and dielectric permittivity, as well as the type of charge storage regulating system—dominant EDLC or pseudo-capacitance. In order to successfully apply and design bimetallic tungstate-based nanobioelectronic devices that advance green technology, our study provides new knowledge [9].

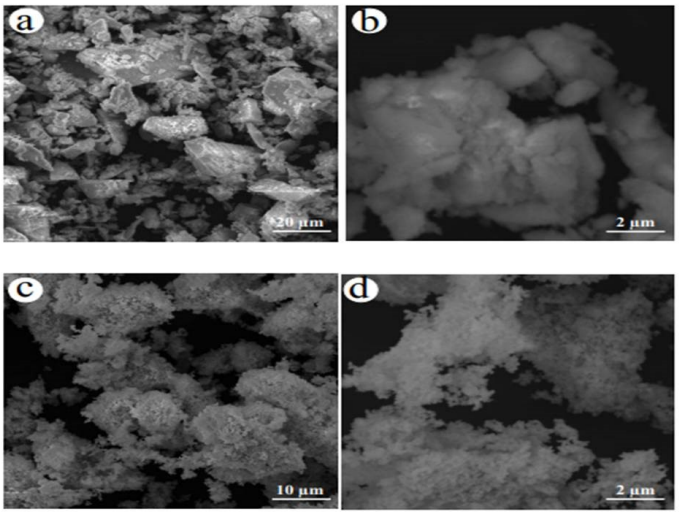

Figure 18: SEM image for; (a) low magnification of $CoWO_4$ (b) high magnification of $CoWO_4$ (c) low magnification of Ni-$CoWO_4$ and (d) high magnification of Ni-$CoWO_4$ [37]

VI. CONCLUSION

In this work, we offer evidence for the synthesis of multi-metallic NPs from diverse plant extracts and the examination of these NPs by UV-vis, XRD, FT-IR, SEM and TEM. In this review, the importance of the optical band supporting photocatalytic activity was described. NPs made from plant extracts have been particularly efficient in decomposing hazardous organic dyes and cleansing contaminated water. Recent breakthroughs in the research of metallic NPs reveal that mixing them with semiconductors is a feasible strategy to build efficient materials that react to visible light. It is realistic to think that such endeavours will permit unfailing success in the development of metallic NPs and make them a key element of visible light photocatalysts. However, they are still inferior in terms of usage and stability. To boost the photocatalytic effectiveness, scavengers must be frequently added to make these photocatalysts photocatalytically stable. In the context of applied nanotechnology, the enhancement of dependable and environmentally acceptable methodologies for the production of metal NPs is a vital step. The future of research should thus concentrate on boosting the production of nanoscale metal particles, the utilisation of inexpensive raw materials and the development of simple energy-saving technologies. As a consequence, it is feasible that the green synthesis of nanoscale metals has extensive applicability and great development potential. We believe that our study will make it easier for young scientists working in this field to comprehend how metal oxide nano particles are generated and employed.

REFERENCES

[1] S. C. Capaldi Arruda, A. L. Diniz Silva, R. Moretto Galazzi, R. Antunes Azevedo, and M. A. Zezzi Arruda, "Nanoparticles applied to plant science: A review," Talanta, vol. 131, pp. 693–705, Jan. 2015, doi: 10.1016/j.talanta.2014.08.050.

[2] H. Mirzaei and M. Darroudi, "Zinc oxide nanoparticles: Biological synthesis and biomedical applications," Ceram. Int., vol. 43, no. 1, pp. 907–914, Jan. 2017, doi: 10.1016/j.ceramint.2016.10.051.

[3] H. Agarwal, S. Venkat Kumar, and S. Rajeshkumar, "A review on green synthesis of zinc oxide nanoparticles – An eco-friendly approach," Resour. Technol., vol. 3, no. 4, pp. 406–413, Dec. 2017, doi: 10.1016/j.reffit.2017.03.002.

[4] H. Abdul Salam, R. Sivaraj, and R. Venckatesh, "Green synthesis and characterization of zinc oxide nanoparticles from Ocimum basilicum L. var. purpurascens Benth.-Lamiaceae leaf extract," Mater. Lett., vol. 131, pp. 16–18, Sep. 2014, doi: 10.1016/j.matlet.2014.05.033.

[5] R. Khursheed et al., "Biomedical applications of metallic nanoparticles in cancer: Current status and future perspectives," Biomed. Pharmacother., vol. 150, p. 112951, Jun. 2022, doi: 10.1016/j.biopha.2022.112951.

[6] S. K. Chandraker, M. K. Ghosh, M. Lal, T. K. Ghorai, and R. Shukla, "Colorimetric sensing of Fe^{3+} and Hg^{2+} and photocatalytic activity of green synthesized silver nanoparticles from the leaf extract of Sonchus arvensis L.," New J. Chem., vol. 43, no. 46, pp. 18175–18183, 2019, doi: 10.1039/C9NJ01338E.

[7] M. Sharma, J. Singh, and S. Basu, "Efficient metal ion adsorption and photodegradation of Rhodamine-B by hierarchical porous Fe-Ni@SiO2 monolith," Microchem. J., vol. 145, pp. 708–717, Mar. 2019, doi: 10.1016/j.microc.2018.11.042.

[8] T. Bavani et al., "One-pot synthesis of bismuth yttrium tungstate nanosheet decorated 3D-BiOBr nanoflower heterostructure with enhanced visible light photocatalytic activity," Chemosphere, vol. 297, p. 133993, Jun. 2022, doi: 10.1016/j.chemosphere.2022.133993.

[9] I. P. Sahu, D. P. Bisen, R. K. Tamrakar, K. V. R. Murthy, and M. Mohapatra, "Luminescence studies on the europium doped strontium metasilicate phosphor prepared by solid state reaction method," J. Sci. Adv. Mater. Devices, vol. 2, no. 1, pp. 59–68, Mar. 2017, doi: 10.1016/j.jsamd.2017.01.001.

[10] B. Parasuraman, B. Kandasamy, V. Vasudevan, and P. Thangavelu, "Enhanced dye degradation performance enabled by swift electron mediator decorated WO3/g-C3N4/V2O5 hybrid nanomaterials," Environ. Sci. Pollut. Res., Jun. 2023, doi: 10.1007/s11356-023-28200-w.

[11] A. N. MARQUES JUNIOR et al., "Tracking atmospheric dispersion of metals in Rio de Janeiro Metropolitan region (Brazil) with epiphytes as bioindicators," An. Acad. Bras. Cienc., vol. 90, no. 3, pp. 2991–3005, Sep. 2018, doi: 10.1590/0001-3765201820170905.

[12] M. G. Neelavannan, M. Revathi, and C. Ahmed Basha, "Photocatalytic and electrochemical combined treatment of textile wash water," J. Hazard. Mater., vol. 149, no. 2, pp. 371–378, Oct. 2007, doi: 10.1016/j.jhazmat.2007.04.025.

[13] A. Akhundi and A. Habibi-Yangjeh, "Ternary g-C3N4/ZnO/AgCl nanocomposites: Synergistic collaboration on visible-light-driven activity in photodegradation of an organic pollutant," Appl. Surf. Sci., vol. 358, pp. 261–269, Dec. 2015, doi: 10.1016/j.apsusc.2015.08.149.

[14] Y. Anjaneyulu, N. Sreedhara Chary, and D. Samuel Suman Raj, "Decolourization of Industrial Effluents – Available Methods and Emerging Technologies – A Review," Rev. Environ. Sci. Bio/Technology, vol. 4, no. 4, pp. 245–273, Nov. 2005, doi: 10.1007/s11157-005-1246-z.

[15] Y. Chang, X. Liu, A. Cai, S. Xing, and Z. Ma, "Glycine-assisted synthesis of mesoporous TiO2 nanostructures with improved photocatalytic activity," Ceram. Int., vol. 40, no. 9, pp. 14765–14768, Nov. 2014, doi: 10.1016/j.ceramint.2014.06.066.

[16] L. S. Cavalcante, J. C. Sczancoski, N. C. Batista, E. Longo, J. A. Varela, and M. O. Orlandi, "Growth mechanism and photocatalytic properties of SrWO4 microcrystals synthesized by injection of ions into a hot aqueous solution," Adv. Powder Technol., vol. 24, no. 1, pp. 344–353, Jan. 2013, doi: 10.1016/j.apt.2012.08.007.

[17] K. N. Kumar, L. Vijayalakshmi, J. Lim, and J. Choi, "Dazzling green luminescent and biocompatible Tb3+ -activated lanthanum tungstate nanophosphors for group-III evaluation of latent fingerprints and anticancer applications," J. Alloys Compd., vol. 959, p. 170415, Oct. 2023, doi: 10.1016/j.jallcom.2023.170415.

[18] A. Elaouni, M. El Ouardi, A. BaQais, M. Arab, M. Saadi, and H. Ait Ahsaine, "Bismuth tungstate Bi_2WO_6: a review on structural, photophysical and photocatalytic properties," RSC Adv., vol. 13, no. 26,

pp. 17476–17494, 2023, doi: 10.1039/D3RA01987J.
[19] V. Sasikala, P. Karthik, S. Ravichandran, N. Prakash, J. Rajesh, and A. Mukkannan, "Effective removal of organic dyes using novel MnWO4 incorporated CA/PCL nanocomposite membranes," Surfaces and Interfaces, vol. 40, p. 103008, Aug. 2023, doi: 10.1016/j.surfin.2023.103008.
[20] R. Surakasi et al., "Methylene Blue Dye Photodegradation during Synthesis and Characterization of WO3 Nanoparticles," Adsorpt. Sci. Technol., vol. 2022, pp. 1–10, Jul. 2022, doi: 10.1155/2022/2882048.
[21] M. Fang, X. Tan, Z. Liu, B. Hu, and X. Wang, "Recent Progress on Metal-Enhanced Photocatalysis: A Review on the Mechanism," Research, vol. 2021, Jan. 2021, doi: 10.34133/2021/9794329.
[22] J. Zhao, C. Chen, and W. Ma, "Photocatalytic Degradation of Organic Pollutants Under Visible Light Irradiation," Top. Catal., vol. 35, no. 3–4, pp. 269–278, Jul. 2005, doi: 10.1007/s11244-005-3834-0.
[23] C. Galindo, P. Jacques, and A. Kalt, "Photodegradation of the aminoazobenzene acid orange 52 by three advanced oxidation processes: UV/H2O2, UV/TiO2 and VIS/TiO2," J. Photochem. Photobiol. A Chem., vol. 130, no. 1, pp. 35–47, Jan. 2000, doi: 10.1016/S1010-6030(99)00199-9.
[24] K. B. Narayanan and N. Sakthivel, "Green synthesis of biogenic metal nanoparticles by terrestrial and aquatic phototrophic and heterotrophic eukaryotes and biocompatible agents," Adv. Colloid Interface Sci., vol. 169, no. 2, pp. 59–79, Dec. 2011, doi: 10.1016/j.cis.2011.08.004.
[25] B. Li et al., "Mesoporous cobalt tungstate nanoparticles for efficient and stable visible-light-driven photocatalytic CO2 reduction," Mater. Today Energy, vol. 24, p. 100943, Mar. 2022, doi: 10.1016/j.mtener.2022.100943.
[26] S. Ghazal, M. Mirzaee, and M. Darroudi, "Green synthesis of tungsten oxide (WO3) nanosheets and investigation of their photocatalytic and cytotoxicity effects," Micro Nano Lett., vol. 17, no. 11, pp. 286–298, Sep. 2022, doi: 10.1049/mna2.12134.
[27] Y. A. Asratemedhin B. Habtemariam, "Synthesis of WO3 Nanoparticles using Rhamnus Prinoides Leaf Extract and Evaluation of its Antibacterial Activities," Biointerface Res. Appl. Chem., vol. 12, no. 1, pp. 529–536, Apr. 2021, doi: 10.33263/briac121.529536.
[28] J. O. Tijani, O. Ugochukwu, L. A. Fadipe, M. T. Bankole, A. S. Abdulkareem, and W. D. Roos, "One-step green synthesis of WO 3 nanoparticles using Spondias mombin aqueous extract: effect of solution pH and calcination temperature," Appl. Phys. A Mater. Sci. Process., vol. 125, no. 3, Mar. 2019, doi: 10.1007/s00339-019-2450-y.
[29] H. V. S. B. Azevêdo et al., "Green synthesis of CoWO4 powders using agar-agar from red seaweed (Rhodophyta): Structure, magnetic properties and battery-like behavior," Mater. Chem. Phys., vol. 242, Feb. 2020, doi: 10.1016/j.matchemphys.2019.122544.
[30] A. Karthika, C. Sudhakar, A. Suganthi, and M. Rajarajan, "Eco-friendly synthesis of aloe vera plant extract decorated iron tungstate nanorods immobilized Nafion for selective and sensitive determination of theophylline in blood serum, black tea and urine samples," J. Sci. Adv. Mater. Devices, vol. 4, no. 4, pp. 554–560, Dec. 2019, doi: 10.1016/j.jsamd.2019.09.004.
[31] B. Fatima, S. I. Siddiqui, R. Ahmed, and S. A. Chaudhry, "Green synthesis of f-CdWO4 for photocatalytic degradation and adsorptive removal of Bismarck Brown R dye from water," Water Resour. Ind., vol. 22, Dec. 2019, doi: 10.1016/j.wri.2019.100119.
[32] R. Karthiga, B. Kavitha, M. Rajarajan, and A. Suganthi, "Photocatalytic and antimicrobial activity of NiWO4 nanoparticles stabilized by the plant extract," Mater. Sci. Semicond. Process., vol. 40, pp. 123–129, Jul. 2015, doi: 10.1016/j.mssp.2015.05.037.
[33] K. Buvaneswari and M. Ganagaraj, "GREEN SYNTHESIS OF NiWO 4 NANOPARTICLES USING PHYLLANTHUS AMARUS EXTRACT."
[34] K. Hkiri, H. E. A. Mohamed, C. B. Mtshali, N. Mongwaketsi, A. Gibaud, and M. Maaza, "Promising photocatalytic activity under visible light of ZnWO4 nanocrystals prepared via green synthesis approach," Mater. Today Commun., vol. 35, p. 106355, Jun. 2023, doi: 10.1016/j.mtcomm.2023.106355.
[35] B. Fatima et al., "Facile green synthesis of ZnO–CdWO4 nanoparticles and their potential as adsorbents to remove organic dye," Environ. Pollut., vol. 271, Feb. 2021, doi: 10.1016/j.envpol.2020.116401.
[36] L. Shiamala, K. Alamelu, V. Raja, and B. M. Jaffar Ali, "Synthesis, characterization and application of TiO2-Bi2WO6 nanocomposite photocatalyst for pretreatment of starch biomass and generation of biofuel precursors," J. Environ. Chem. Eng., vol. 6, no. 2, pp. 3306–3321, Apr. 2018, doi: 10.1016/j.jece.2018.04.065.
[37] S. Jha, S. Mehta, E. Chen, S. S. Sankar, S. Kundu, and H. Liang, "Bimetallic tungstate nanoparticle-decorated-lignin electrodes for flexible supercapacitors," Mater. Adv., vol. 1, no. 6, pp. 2124–2135, 2020, doi: 10.1039/d0ma00494d.
[38] U. Baig, M. A. Gondal, S. Rehman, and S. Akhtar, "Facile synthesis, characterization of nano-tungsten

trioxide decorated with silver nanoparticles and their antibacterial activity against water-borne gram-negative pathogens," Appl. Nanosci., vol. 10, no. 3, pp. 851–860, Mar. 2020, doi: 10.1007/s13204-019-01186-z.

[39] G. Duan et al., "Robust Antibacterial Activity of Tungsten Oxide (WO_{3-x}) Nanodots," Chem. Res. Toxicol., vol. 32, no. 7, pp. 1357–1366, Jul. 2019, doi: 10.1021/acs.chemrestox.8b00399.

[40] Z. Gu et al., "Large-scale synthesis of single-crystal hexagonal tungsten trioxide nanowires and electrochemical lithium intercalation into the nanocrystals," J. Solid State Chem., vol. 180, no. 1, pp. 98–105, Jan. 2007, doi: 10.1016/j.jssc.2006.09.020.

[41] N. S. Kavitha, K. S. Venkatesh, N. S. Palani, and R. Ilangovan, "Fungus mediated biosynthesis of WO3 nanoparticles using Fusarium solani extract," 2017, p. 050130. doi: 10.1063/1.4980363.

[42] Karthiga Rajendaran and Sudha Annamalai1, "Green Synthesis of ZnO Nanoparticles Using Sollanam Santhocarbom to Study Its Solarphotocatalytic Activity," Int. J. Sci. Res., vol. 6, no. 6, pp. 2370–2376, Jun. 2015.

[43] A. Mohamed Azharudeen, R. Karthiga, M. Rajarajan, and A. Suganthi, "Enhancement of electrochemical sensor for the determination of glucose based on mesoporous VO2/PVA nanocomposites," Surfaces and Interfaces, vol. 16, pp. 164–173, Sep. 2019, doi: 10.1016/j.surfin.2019.05.005.

[44] A. Mohamed Azharudeen, R. Karthiga, M. Rajarajan, and A. Suganthi, "Selective enhancement of non-enzymatic glucose sensor by used PVP modified on α-MoO3 nanomaterials," Microchem. J., vol. 157, p. 105006, Sep. 2020, doi: 10.1016/j.microc.2020.105006.

[45] A. M. Azharudeen et al., "Ultrasensitive and Selective Electrochemical Detection of Dopamine Based on CuO/PVA Nanocomposite-Modified GC Electrode," Int. J. Photoenergy, vol. 2022, pp. 1–9, Feb. 2022, doi: 10.1155/2022/8755464.

[46] R. Karthiga, B. Kavitha, M. Rajarajan, and A. Suganthi, "Synthesis of MoO3 microrods via phytoconsituents of Azadirachta indica leaf to study the cationic dye degradation and antimicrobial properties," J. Alloys Compd., vol. 753, pp. 300–307, Jul. 2018, doi: 10.1016/j.jallcom.2018.04.230.

[47] A. M. Azharudeen et al., "Solar Power Light-Driven Improved Photocatalytic Action of Mg-Doped CuO Nanomaterial Modified with Polyvinylalcohol," J. Nanomater., vol. 2022, pp. 1–15, Mar. 2022, doi: 10.1155/2022/2430840.

[48] B. Fatima et al., "Photocatalytic removal of organic dye using green synthesized zinc oxide coupled cadmium tungstate nanocomposite under natural solar light irradiation," Environ. Res., vol. 216, p. 114534, Jan. 2023, doi: 10.1016/j.envres.2022.114534.

[49] K. Hkiri, H. E. A. Mohamed, C. B. Mtshali, N. Mongwaketsi, A. Gibaud, and M. Maaza, "Promising photocatalytic activity under visible light of ZnWO4 nanocrystals prepared via green synthesis approach," Mater. Today Commun., vol. 35, p. 106355, Jun. 2023, doi: 10.1016/j.mtcomm.2023.106355.

[50] K. Buvaneswari, R. Karthiga, B. Kavitha, M. Rajarajan, and A. Suganthi, "Effect of FeWO 4 doping on the photocatalytic activity of ZnO under visible light irradiation," Appl. Surf. Sci., vol. 356, pp. 333–340, Nov. 2015, doi: 10.1016/j.apsusc.2015.08.060.

[51] A. Sarwar, A. Razzaq, M. Zafar, I. Idrees, F. Rehman, and W. Y. Kim, "Copper tungstate (CuWO4)/graphene quantum dots (GQDs) composite photocatalyst for enhanced degradation of phenol under visible light irradiation," Results Phys., vol. 45, p. 106253, Feb. 2023, doi: 10.1016/j.rinp.2023.106253.

[52] I. Arora, H. Chawla, A. Chandra, S. Sagadevan, and S. Garg, "Advances in the strategies for enhancing the photocatalytic activity of TiO2: Conversion from UV-light active to visible-light active photocatalyst," Inorg. Chem. Commun., vol. 143, p. 109700, Sep. 2022, doi: 10.1016/j.inoche.2022.109700.

[53] Y. M. Lee and C. H. Lai, "Preparation and characterization of solid n-TiO2/p-NiO hetrojunction electrodes for all-solid-state dye-sensitized solar cells," Solid. State. Electron., vol. 53, no. 10, pp. 1116–1125, Oct. 2009, doi: 10.1016/j.sse.2009.07.004.

[54] R. Arunadevi, B. Kavitha, P. P. Sudha, M. Rajarajan, and A. Suganthi, "Photocatalytic enhancing for tin oxide nanoparticles by codoping with nitrogen and bismuth," Desalin. Water Treat., vol. 78, pp. 330–340, Jun. 2017, doi: 10.5004/dwt.2017.20773.

